PROTON RESONANCES IN NATURAL SILICON

WILLIAM C. ROBERTS, JR.
AND
D. HUNT WILLIAMS

54

PROTON RESONANCES IN NATURAL SILICON

* * * * *

William C. Roberts, Jr.

and

"D" Hunt Williams

PROTON RESONANCES IN NATURAL SILICON

by

William C. Roberts, Jr.
Captain, United States Marine Corps

and

"D" Hunt Williams
Lieutenant Commander, United States Navy

Submitted in partial fulfillment of
the requirements for the degree of

MASTER OF SCIENCE
IN
PHYSICS

United States Naval Postgraduate School
Monterey, California

1 9 5 8

PROTON RESONANCES IN NATURAL SILICON

by

William C. Roberts, Jr.

and

"D" Hunt Williams

This work is accepted as fulfilling
the thesis requirements for the degree of

MASTER OF SCIENCE

IN

PHYSICS

from the

United States Naval Postgraduate School

ABSTRACT

Proton resonances in natural silicon were investigated using a proton beam from the 2-Mev Van de Graaff accelerator at the U. S. Naval Postgraduate School. A single crystal of high purity natural silicon was bombarded by protons with energies in the range 900 to 1800 kev. The gamma-ray yield, with contributions from positron decay of P^{29} and P^{30}, was observed as a function of proton energy for two integral amplifier bias settings of 1.8 and 3.0 Mev as well as one differential bias from 0.45 Mev to approximately 1.45 Mev. The proton energy was measured by means of a magnetic analyzer. Resonances were found at proton energies of 944, 988, 1035, 1076, 1104, 1171, 1214, 1294, 1310, 1334, 1377, 1399, 1407, 1488, 1498, 1518, 1527, 1531, 1655, 1695, 1755, and 1781 kev. On the basis of observed half-life, the 1655 kev resonance was assigned to the $Si^{28}(p,\gamma)P^{29}$ reaction.

The writers wish to express their appreciation for the assistance and encouragement given them by Professor Edmund A. Milne in this investigation as well as to Kenneth C. Smith who provided assistance in the maintenance of electronic equipment.

This project was supported in part by the Office of Naval Research.

TABLE OF CONTENTS

LIST OF ILLUSTRATIONS

Figure

1. Introduction

This investigation was conducted to determine resonances in the $Si(p, \gamma)P$ reactions attainable by bombardment of a high purity single crystal of natural silicon with protons of energies in the range 900 to 1800 kev.

Proton bombardment of the Si^{28}, Si^{29}, and Si^{30} nuclides found in natural silicon can produce simple proton capture reactions resulting in the formation of excited compound nuclei of P^{29}, P^{30} and P^{31} respectively, which decay to ground states by gamma-ray emission. Excitation curves were constructed from data obtained by measuring gamma-ray intensities at discrete proton bombarding energies. The curves presented resonance "steps" characteristic of thick target response.

The nuclides P^{29} and P^{30} are radioactive, decaying by β^+ emission with half-lives of 4.6 seconds and 2.5 minutes respectively. Use of this phenomena was made in the isotopic assignment of a resonance to the $Si^{28}(p, \gamma)P^{29}$ reaction.

2. Historical Background

During the early 1930's the experiments of Curie and Joliot involving the exposure of B^{10} to alpha rays from polonium resulted in the discovery of N^{13} and led to their suggestion that their newly discovered isotope could probably be produced by deuteron bombardment of carbon. This suggestion was promptly verified by M. C. Henderson, et al (1), at Berkley and by H. R. Crane, et al (2), at Pasadena where deuteron beams were available. It began to be recognized that nuclear reactions might involve the formation of an intermediate nucleus. With the

development of various types of particle accelerators, there followed many rapid advances in the theoretical understanding of nuclear reactions, among which was the development of the compound nucleus concept by Bohr [3] and, independently, by Breit and Wigner [4] . An extended analysis of the concept of the compound nucleus has been given by Blatt and Weisskopf [5] . In essence, the concept postulated that the same compound nucleus could be formed in a variety of ways. For instance, the compound nucleus N^{14} could result from

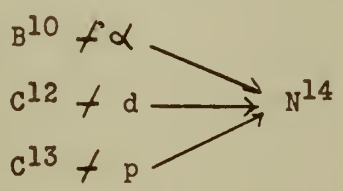

Once formed, the compound nucleus would have a lifetime which would be very long ($\sim 10^{-16}$ sec.) compared with the time required for a proton to cross the nucleus ($\sim 10^{-22}$ sec.) and the final products of the reaction would be independent of the manner in which the compound nucleus was formed. For example, N^{14} might dissociate in any of several competing ways such as

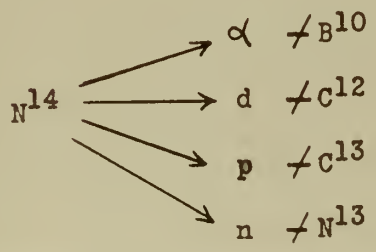

This concept, later verified by many investigators, and the rapid improvement of particle accelerators opened the way for experimental accumulation of information pertaining to nuclear energy levels and decay schemes. Subsequent work has progressed at a rapid pace and the accumulation of data mounts at an ever-increasing rate during the present time.

3. Proton Resonance Phenomena

When a nucleus is bombarded by a proton, the particle may merely be elastically scattered or it may be captured by the target nucleus and a compound nucleus formed. In order to form a compound nucleus, the proton must penetrate the coulomb barrier and also the nuclear "surface." According to quantum theory analysis, a detailed presentation of which has been given by Evans (6) , the probability of transmission through the potential step at the nuclear surface is usually not a monotonic function of the bombarding energy. Instead, there are particular values of the incident energy for which the probability of formation of the compound nucleus is largest. If the excitation energy of the compound nucleus, determined by the masses of the colliding nuclei plus the incident kinetic energy in the center-of-mass coordinates, is just equal to that of one of the quantum excited states, and if angular momentum, etc. are "right," a large reaction probability for formation of the compound nucleus exists. The discrete proton energies at which the high reaction probability occurs are called "resonance energies" or "resonances." An extended analysis of the resonance phenomena has been given by Fowler, et al (7) .

The excited compound nucleus formed in the reaction may decay in a number of different ways. If the decay is by gamma-ray emission, the discrete energy states of the compound nucleus can be determined experimentally by measurement of gamma-ray intensity at varying proton energies. The energy level of the compound nucleus formed corresponding to a particular proton resonance energy is given, in Mev, by

$$E = Q + \frac{M}{m + M} E_p$$

where Q is the Q of the reaction, M is the mass of the target nucleus, m is the mass of the proton, and E_p is the kinetic energy of the proton in laboratory coordinates.

4. Proton Reactions in Silicon

Natural silicon is composed of the following three isotopes:

Isotope	Percentage (Wt.)
Si^{28}	92.21
Si^{29}	4.70
Si^{30}	3.09

Bombardment of any of the three silicon isotopes by protons in the energy range considered in this investigation can result in the formation of excited compound nuclei which can decay only by gamma-ray emission. Table I shows that proton capture reactions involving decay by emission of α, d, or n are energetically impossible in this bombarding energy range since the Q values for the initial reactions are negative and of magnitude greater than 2.376 Mev.

Gamma-ray emission may also result from inelastic scattering. In order for a proton to be inelastically scattered, it must be absorbed by a target nucleus at one of the discrete nuclear energy levels. The lowest levels of the three isotopes of silicon are as follows (8) :

Isotope	Energy Level
Si^{28}	1.78 Mev
Si^{29}	1.28 Mev
Si^{30}	2.24 Mev

At proton energies below 1800 kev (laboratory coordinates), inelastic scattering is possible only in the case of Si^{29}. Since the probability

of this phenomenon is low, in the energy range 1320 to 1800 kev, the contribution to gamma-ray yield by inelastic scattering was considered insignificant.

5. Previous Investigations in Silicon

The first reported determination of proton resonances in natural silicon were made by Hole, Holtsmark and Tangen (9) who detected resonances in the gamma-ray yield at proton energies of 413 and 419 kev. Later, Tangen (10) bombarded both thick and thin targets and reported resonances which he assigned to the separate silicon isotopes as follows:

Resonance Energy (kev)	Isotope
326	Si^{29}
367	Si^{30}
414	Si^{29}
499	Si^{30}

In 1955, Seiler (11) reported resonances in natural silicon at proton energies of 622, 675, 698, 703, 732, 760, 778, 944 and 989 kev obtained using the Van de Graaff accelerator at Ohio State University. Later investigations at this institution were reported in 1956 by Milani, Cooper and Harris (12) in which thick and thin targets of Si^{29}, enriched to 80.8 per cent, were bombarded by protons in the energy range of 250 to 1300 kev and resulted in determination of resonances at 326, 414, 698, 731, 918, and 957 kev.

Many investigations have been conducted since 1956 using targets of natural silicon and of separated isotopes. A comprehensive review and evaluation of the accumulated data has been given by P. M. Endt and C. M. Braams (8) .

Recent investigations were conducted by N. K. Green and R. F.

Wiseman (13) in which thin targets of both natural silicon and of separated isotopes were bombarded with protons in the energy range of 850 to 2030 kev. They determined 36 resonances in natural silicon in the range of proton energies considered by this report and assigned 11 resonances to the $Si^{29}(p,\gamma)P^{30}$ reaction, and 25 to the $Si^{30}(p,\gamma)P^{31}$ reaction. No resonances due to the $Si^{28}(p,\gamma)P^{29}$ reaction were observed. Table II contains a summary of the resonances reported to date in the energy range, 900 to 1800 kev (laboratory coordinates). Where resonance energies reported by separate investigators have been determined to be in near agreement, all reported energies have been listed as a single resonance and bibliography references given in the order in which the corresponding energy appears. With the exception of the Si^{28} resonance at 1650 kev (8), the isotopic assignments and values of relative yield and experimental half-width listed in Table II are those reported by Green and Wiseman.

6. Equipment

The 2-Mev horizontal Van de Graaff electrostatic accelerator, (Model H/S HVI-34, High Voltage Engineering Corporation) was used to provide a focused beam of energetic protons for target bombardment during this investigation. The accelerator installation consisted of the following major sections:

a. The Accelerator Section

The accelerator section, enclosed in a steel housing pressurized with nitrogen-carbon dioxide gas mixture, contained components for the production and acceleration of particles. Protons of masses one, two and three were produced by radio-frequency ionization of

hydrogen gas in a manner similar to that comprehensively described by C. D. Moak, et al [14] .

b. The Analyzer Section

The analyzer section consisted of a 25-degree magnetic analyzer through which the proton beam was passed in order to select particles of a desired mass and energy for target bombardment.

c. The Target Section

The target section (Fig. 1) contained energy defining slits, through which the proton beam was received from the analyzer section, a beam shutter and the target chamber. The slits, located at a distance of 2.1 meters from the center of the analyzer magnet, served the dual purpose of defining the energy width of the proton beam and feeding back, via electronic circuitry, beam stabilizing signals to the accelerator section.

The target chamber was designed and constructed to provide rapid and easy access for changing targets, integration of target bombarding charge, and maximum gamma-ray detection efficiency. It consisted of a metal section terminated with a high-vacuum metal-to-glass coupling to which was fitted a 7.8 cm long glass cap ($\frac{1}{2}$" O.D.). The glass cap served as an electrically insulated target housing of appropriate diameter to fit deeply inside a well-type NaI(Th) scintillation crystal. A silver wire was brought into the metal chamber using a Kovar glass seal and was insulated with glass beads in order to allow laying the wire along the chamber wall insuring ample clearance from the proton beam path. A groove was cut in the lip of the metal-to-glass coupling at the point of juncture with the rim of the glass cap. To provide insulation and rigid support for the wire, glass beads were cemented in the groove using red glyptal. The silver wire was led into the glass cap and positioned to

lie in contact with the cap wall, again, to provide beam-path clearance. A target mount was made from hammered silver wire and fastened to the supporting silver wire by means of a small-diameter quick-disconnect male-female fitting. The opposite end of the support wire was connected to a current integrating circuit.

A second silver wire was similarly passed into the metal section and formed into a loop, encompassing but well clear of the proton beam. The initial end of the wire was passed through a 10 megohm resistor to the negative terminal of a 300 volt dry cell battery with the positive terminal grounded to the external chamber wall. This provided a Faraday Cage for the purpose of repelling negative ions formed upstream of the loop by ionization of residual gas molecules and preventing escape of electrons from the target.

The target section was equipped with an auxiliary fore-pump and diffusion-pump system with valves which permitted isolation of the target chamber, rapid installation or change of targets, separate fore-pump roughing, and the resumption of operation with a minimum of delay since it was not necessary to disturb the vacuum in the remainder of the accelerator.

d. The Control Console

The control console was located in a separate room from the accelerator to provide remote control from a shielded area which was necessary for personnel protection from radiation hazard when the machine was operated in the electron-accelerator configuration. The console contained elements for the selection and control of accelerating voltage and analyzer magnet current. A Leeds and Northrup potentiometer was added as as auxiliary console equipment for the precise measurement of magnet

current, and hence, precise selection of proton energy. Coordination between the control room and the accelerator room was provided by a typical office intercommunication system.

e. The Auxiliary Section

The auxiliary section of the installation included components for the control of bombardment parameters and detection of target yield. The gamma-ray yield was detected by a two-inch diameter, well-type, thallium-activated sodium iodide crystal mounted on a photomultiplier tube (Fig. 2). Signals from the photomultiplier were passed to two non-overloading linear amplifiers, one of which was equipped with differential pulse height discrimination. After amplification the signals were passed to two separate scalers for counting. Signal monitoring was provided by passing undiscriminated signals from both amplifiers to separate input terminals of a cathode ray oscilloscope.

To control bombardment parameters, the target current integrator circuitry was arranged to provide, through a manual switch, the simultaneous starting and stopping of bombardment, scalers and a timer. Closing the manual switch activated relays which started the scalers and the timer and, at the same time, opened a solenoid operated beam shutter. At the completion of a period of bombardment, determined by the target current integrator, relays stopped the timer and scalers and closed the beam shutter. An additional manual switch was provided to control the beam shutter independently of current integrator operation for use in beam focusing and target alignment. The beam shutter furnished a method of avoiding continuous target bombardment with attendant target heating and deterioration during intervals between measurements.

7. Experimental Procedure

The operation of the accelerator was conducted by the coordinated effort of the two-man team. One man was stationed at the console to control the operation of the accelerator and the magnetic analyzer. Prior to commencing an investigative operation, the magnet current was cycled twice through its complete range in order to minimize the hysteresis effect. Once an operation was commenced, the magnet-current control was always moved only in the direction of increasing magnet current thereby providing operation on a single hysteris loop throughout the operation. At each step the magnet current was measured by means of the potentiometer which was checked against a standard cell.

The second member of the team was stationed adjacent to the target section and controlled the bombardment and detection equipment by means of the manual "start" switch on the target-current integrator. The duration of a period of bombardment was controlled by selection of the combination of integrator-capacitor and beam-current magnitudes appropriate for achieving maximum target bombardment rate compatible with limitations imposed by allowable target heating. Beam current and corona stabilizer balance meter readings were relayed via the intercommunication system to the console operator to assist in control of the accelerator. At the end of each bombardment period, the target-section member recorded readings of the scalers, timer, beam-current meter, and the corresponding magnet current reading furnished by the console operator.

Before commencing the investigation of silicon, thin targets were made by vacuum evaporation of LiF onto thin tantalum disks. The prominent $F^{19}(p,\gamma)Ne^{20}$, $F^{19}(p,\alpha)O^{16}$ resonances and the $Li^{7}(p,n)Be^{7}$

threshold (19) were used for calibration of the accelerator and a curve of proton-energy versus magnet current was plotted for use in preliminary work. Later, use was made of the quick-target-change feature of the target chamber to permit calibration during an operation since calibration was found to shift linearly between separate investigations due to analyzer magnet hysteris effect.

The linear amplifiers were biased and the oscilloscope calibrated prior to each operation by use of the 1.11 Mev gamma ray from a Zn^{65} source.

The target used in this project was made by cutting a 7.7 x 6.4 x 1.4 millimeter block from a single crystal of high purity (99.9%), transistor grade, natural silicon.

The procedure employed during the investigation of a particular proton energy range consisted of advancing the magnet current in increments of approximately .002 amp. corresponding to proton energy steps of approximately 3.3 kev (laboratory coordinates). Bombardment periods were of 30 seconds duration, on the average, although this varied to some extent between separate investigations since the parameter held constant throughout the entire project was that of bombardment charge (number of protons). At each magnet current setting, the yield was measured during a minimum of three bombarding periods with additional periods used where comparison of the three separate scaler readings resulted in a count variation range in excess of $2 \cdot x \sqrt{count}$.

An operation was always terminated by traversing a prominent pair of resonances which, by starting at a lower energy on a subsequent operation, allowed determination of the linear calibration shift and

afforded continuity of investigation through the entire proton-energy range studied.

Radio-active product nuclei half-lives were determined as follows: In order to achieve a high production rate of short half-life nuclei, the target was bombarded with the maximum obtainable beam current. Bombardment was terminated by cutting off the beam at the accelerator section and, at the same time, the scaler was started. During half-life determination, the amplifier in use was biased below .511 Mev to detect annihilation radiation. Counts were obtained during five second counting periods separated by five second intervals. After readings were corrected for coincidence losses, a graph of "Ln Count" versus "Elapsed Time" was constructed and the decay constant determined.

8. Interpretation of Data

In the thick target excitation curves obtained from the experimental data, the presence of resonances was indicated by relatively sharp rises in yield from a general level. This was complicated by a gradual quasi-exponential rise in background where the selected amplifier bias permitted acceptance of energy pulses below approximately 4 Mev. This rise was caused by the production of a positron emitter, P^{30}, with end point energy of about 4 Mev which produced bremmstrahlung and annihilation radiation upon decay. The larger-yield resonances were presented clearly, but in the case of smaller-yield resonances, the criteria of sharp "breaks" in the slope of the curve was used for resonance determination and location with apparently consistent results.

Data was obtained with integral bias settings of 1.8 Mev and 3.0 Mev and with a differential bias from .45 Mev to approximately 1.45 Mev,

hereinafter referred to as the ".511 Mev bias." The latter included yield contributions from low-energy gamma, bremmstrahlung and positron annihilation radiation. From the excitation data and half-life-determination data obtained with the .511 Mev bias it appeared that this setting was effective in recording high-yield, lower-gamma-energy resonances. Because of the large gamma contribution during bombardment, the yield was largely unaffected by the relatively long-lived positron emitter. To obtain an estimate of the order of magnitude of these effects, the count rate was noted during a bombardment at an intermediate proton energy (about 1500 kev). It was determined to be approximately 1000 counts per second, while a decay count immediately following produced an initial count rate of only about 50 counts per second.

The detailed shape of a resonance of appreciable width appeared as a roughly "S" shaped curve. The height of the step, or count increase, between 10% and 90% of the total rise was selected as the criteria for estimation of resonance yield, based upon considerations of accuracy and reproducibility. The relative yield values obtained were based on one relative-yield unit corresponding to 1,000 counts during an approximately 30 second bombardment period. The width of a resonance was determined from the difference between the proton energy values of the 10% and 90% points. The energy value of a resonance, E_p, was determined as the energy corresponding to the 50%-of-rise point.

A thick target resonance response is an integration of the corresponding thin target resonance response and the two curves have the same relation as a distribution function and its related integral curve. A consideration of similarly appearing curves, i.e., the normal

distribution curve and its related integral curve, led to the conclusion that the resulting widths as determined above should be in rather close agreement with the corresponding widths of thin target resonances obtained at half of the height.

The apparent width of a resonance is effected by the stability and energy resolution of the bombarding beam. The stability or regulation of beam energy was stated by the accelerator manufacturer to be about ± 2 kev in the range of energies utilized. The beam defining slits were adjusted to a relatively wide spacing ($\sim$ 3 mm.) during this investigation and it is believed that the degradation of energy resolution contributed approximately 2 kev to the apparent width of the resonances.

9. Results

Figure 4 is a reproduction of the natural silicon thin target excitation curve which resulted from the work of Green and Wiseman [13] . This curve is a graph of relative yield (arbitrary units) versus proton energy (laboratory coordinates), including background, and is presented in this report for comparison with thick target excitation curves resulting from this investigation.

The thick target excitation curves obtained in this project are presented in Figures 5, 6, and 7. Fig. 5 shows the excitation curves representing the entire energy range investigated and, for comparison, was plotted to the same proton energy scale as that used in Fig. 4, although the relative-yield scales of the two illustrations were unrelated. Portions of these curves are shown in expanded presentations in Figures 6 and 7 for particular proton-energy ranges. The expanded curves include loci of the smooth data points used in the curve construction. The "bias" value shown on a particular curve indicates the particular amplifier bias setting used in obtaining the data from which the curve resulted. The 0.511 Mev bias curve was plotted at one-tenth actual yield values because of the large number of counts obtained at this bias. The resonances shown on this curve, however, were of the same order of magnitude as those on the other curves.

The resonance energies determined in this investigation, together with corresponding relative yields and experimental widths, are shown in

Table III. For convenience of cross reference to pertinent sections of the excitation curves, the discussion of individual resonances has been divided into the following sections corresponding to particular ranges of proton energy:

a. 900 to 1300 kev

Eight resonances were observed in this region at proton energies, E_p, of 944, 988, 1035, 1076, 1104, 1171, 1214, and 1294 kev. Several resonances observed on the .511 Mev bias curve were not detected on the 3.0 Mev curve. In general, agreement between values of proton energy determined for resonances detected on both curves was good. The 0.511 Mev bias data contained considerably greater statistical fluctuation which made the determination of resonance width very difficult and, in general, these values were considered less reliable than those based on the high bias curve.

b. 1300-1500 Kev

Ten resonances were observed in this energy range at proton energies of 1310, 1334, 1377, 1399, 1407, 1488, 1498, 1518, 1527 and 1531 kev. Values of resonance energy, relative yield and resonance width were determined from the three curves of 0.511, 1.8 and 3.0 Mev bias in the energy range 1300-1350 kev (Fig. 6). Above 1350 kev large statistical fluctuations in the 0.511 data invalidated general use of this curve for other than verification of presence of a resonance primarily detected on the other two curves.

The resonance at 1377 kev was detected on the 3.0 Mev bias curve but was observed as a general rise in the 1.8 Mev bias curve which was insufficiently resolved to indicate the exact resonance energy.

Presence was confirmed by the 0.511 Mev bias curve.

The 1399 and 1407 kev resonances were observed as two distinctly separate rises on the 1.8 Mev bias curve while the 3.0 Mev bias curve showed a single unresolved rise, centered at 1404 kev which was apparently due to the two resonances.

At energies above 1450 kev, a large increase in statistical fluctuation in the 1.8 Mev bias data made it unreliable for resonance determination and its further use for this purpose was abandoned.

c. 1550-1700 kev

The results achieved in this energy range proved to be the most significant of the observations made during the investigation. The excitation curves for the proton energy range 1600 to 1700 kev, clearly shown in Figures 5 and 7, were dominated by a large, steep rise which was an order of magnitude greater than any of the resonances previously observed. Based upon consideration of the "breaks" in the slope of the excitation curves, as discussed in the previous section, the resonance was centered at 1665 kev and had a width of approximately 50 kev. A half-life count obtained after bombardment of the target at 1700 kev E_p revealed the presence of two different activities with half-lives of approximately 2.9 minutes and 5 seconds. Half-life determination made at proton energies below 1600 kev showed the presence of the longer half-life nuclide only. Since the accepted half-life values for P^{29} and P^{30} are 4.5 seconds and 2.55 minutes respectively [8] , the 1665 kev resonance was assigned to the $Si^{28}(p,\gamma)P^{29}$ reaction.

The resonance at 1695 kev was observed on the 0.511 Mev bias curve but was unresolved in the previously mentioned large rise of the 3.0 Mev

bias curve. At 1755 kev a resonance was observed on the 3.0 Mev bias curve but, unlike any previous resonances, failed to be indicated on the 0.511 Mev bias curve. A second investigation through this energy range reproduced this resonance on the 3.0 Mev bias for verification.

The apparent fluctuations in the 3.0 Mev bias curve in the energy range 1710 to 1740 kev were reproducible and were considered to be the result of target surface contamination producing a thin-target type of resonance pattern. The nature of the contamination was not determined.

10. Conclusions

The experimental results of this investigation have been presented in Table III. Comparison with Table II, representing previous work, shows excellent agreement in general. The average deviation from previously determined values was on the order of 2 kev, with the exception of the three resonances at 1035, 1076 and 1531 kev. The maximum deviation from previous assignments was 7 kev for the 1171 kev resonance. On the basis of this observation and the accelerator manufacturer's claim pertaining to machine energy resolution, an error of ± 2 kev in the resonance energy assignments was considered appropriate.

From considerations of energy stability and beam energy definition, it was concluded that at least 2 kev of the observed widths was attributable to these factors.

A complete interpretation of resonance phenomena displayed by a thick target requires the consideration of a number of factors. The response observed, i.e., relative yield, at particular resonances is dependent not only upon the magnitude of the probability of compound nucleus formation and upon the detection resolution, but also is largely

a function of the decay scheme of the particular level. As shown in the results of this investigation, the use of various bias levels is necessary for the detection of various resonances because of the differences in gamma-cascade energies and background-determined resolution requirements. A multi-channel analyzer would provide, in future investigations, an economical means of greatly increasing the scope of the investigation.

An additional complicating factor is introduced, in the accurate determination of resonances, by the formation of radioactive product nuclei. At bias settings corresponding to energies less than that required to reject the yield contributions of the emitted particles, i.e., bremsstrahlung and annihilation radiation, there may be unavoidable failure to detect low-yield-gamma resonances because of the statistical fluctuations caused by differences of time between observations. Future investigators, however, may find it useful to employ a differential bias of least practicable energy-width solely for the detection of the 0.511 Mev annihilation radiation produced in positron decay.

From consideration of the 1600 to 1700 kev region displayed in Figure 4 it appears that the previous investigation by Green and Wiseman [13] did, in fact, detect the 1655 kev resonance attributable to $Si^{28}(p,\gamma)P^{29}$ but the rise in the excitation curve in this region was interpreted as being caused by target contamination by C^{12} producing a broad resonance at about 1690 kev.

BIBLIOGRAPHY

1. M. C. Henderson, M. S. Livingston, and E. O. Laurence: Phys. Rev. 45, 428L (1934).

2. H. R. Crane and C. C. Lauritsen: Phys. Rev. 45, 430L, 497L (1934).

3. N. Bohr: Nature 137, 344 (1936).

4. G. Breit and E. Wigner: Phys. Rev. 49, 519 (1936).

5. J. M. Blatt and V. F. Weisskopf: Theoretical Nuclear Physics, John Wiley & Sons, (1952).

6. R. D. Evans: The Atomic Nucleus, McGraw-Hill Inc., (1955).

7. W. A. Fowler, C. C. Lauritsen, and T. Lauritsen: Rev. Mod. Phys. 20, 236 (1948).

8. P. M. Endt and C. M. Braams: Rev. Mod. Phys., 29, 683 (1957).

9. N. Hole, J. Holtzmark, and R. Tangen: Z. F. Phys. 181, 48 (1941).

10. R. Tangen: Kgl. Norske Videnskab. Selskabs, Skrifter, NR 1 (1946).

11. M. R. Seiler: M. S. Thesis, Ohio State U., 1955 & Phys. Rev. 99, 340 (1955).

12. S. Milani, J. N. Cooper, and J. C. Harris: Phys, Rev. 99, 645 (1955).

13. N. K. Green and R. F. Wiseman: M. S. Thesis, U.S.N.P.G.S., (1958).

14. C. D. Moak, H. Reese, Jr., and W. M. Good: Nucleonics 9, No. 3, 18 (1951).

15. P. M. Endt and J. C. Kluyver: Rev. Mod. Phys. 26, 95 (1954).

16. C. Broude, L. L. Green, J. J. Singh, and J. C. Willmott: Phys. Rev. 101, 1052 (1956)

17. L. W. Seagondollar, J. A. Woods, H. G. DeSouza and W. A. Glass: Bulletin of the Am. Phys. Soc. Ser. II, Vol. 2, No. 6, 304 (1957).

18. S. P. Tsytko and Iv. P. Antuf': J. Exptl. Theoret. Phys. (USSR) 30, 1171 (June 1956).

19. F. Ajzenberg and T. Lauritsen: Rev. Mod. Phys. 27, 77 (1955).

Proton Reactions in Silicon

Reaction	Q (Mev)	Bibliography Reference
$Si^{28}(p,\gamma)P^{29}$	2.724	15
$Si^{29}(p,\gamma)P^{30}$	5.562	8
$Si^{30}(p,\gamma)P^{31}$	7.292	8
$Si^{28}(p,n)P^{28}$	-14.6	8
$Si^{29}(p,n)P^{29}$	- 5.750	8
$Si^{30}(p,n)P^{30}$	- 5.047	8
$Si^{28}(p,d)Si^{27}$	-14.951	8
$Si^{29}(p,d)Si^{28}$	- 6.246	16
$Si^{30}(p,d)Si^{29}$	- 8.388	16
$Si^{28}(p,\alpha)Al^{25}$	- 7.71	8
$Si^{29}(p,\alpha)Al^{26}$	- 4.816	8
$Si^{30}(p,\alpha)Al^{27}$	- 2.376	8

Table I

Silicon Resonances From Previous Investigations
(900 to 1800 kev)

E_p (lab)	Isotopic Assignment	Relative Yield	Experimental Half-Width	Bibliography Reference
920,916,918	Si^{29}	150	5.0	13,8
940	Si^{30}			18
945	Si^{30}	600	4.0	13,11,17
955	Si^{30}			8
960,956,957	Si^{29}	70	6.5	13,8,12
980	Si^{30}			17,18
989	Si^{30}	680	3.3	13,11
995	Si^{30}			8
1000	Si^{30}			8
1108	Si^{30}	150	4.1	13
1178	Si^{30}	600	4.8	13
1188	Si^{30}	200	3.5	13
1202				17
1205				17
1214	Si^{30}	1180	3.2	13
1221	Si^{30}	500	4.3	13
1263	Si^{30}	480	4.1	13
1297,1291	Si^{30}	270	3.3	13,17
1303	Si^{30}	420	3.2	13
1307	Si^{30}	500	4.5	13
1309	Si^{29}	470	5.4	13
1329,1327	Si^{30}	1490	4.3	13,17

Table II

Table II (Continued)

1334	Si^{29}	800	6.9	13
1353	Si^{30}	270	3.8	13
1379	Si^{30}	220±50	3.0±1.0	13
1397,1394	Si^{30}	1720	2.5	13,17
1406	Si^{30}	1600	2.1	13
1425	Si^{30}	240	2.7	13
1479	Si^{29}	300	5.0	13
1491	Si^{30}	1850	3.1	13
1498	Si^{30}	1100	2.4	13
1515	Si^{29}	1380	5.0	13
1519,1520	Si^{30}	1400	2.6	13,18
1526	Si^{30}	200	3.7	13
1606	Si^{30}	280	2.1	13
1618				18
1635				18
1648,1647	Si^{29}	300	8.3	13,18
1650	Si^{28}		50.5	8
1667,1663	Si^{30}	270	2.5	13,18
1671	Si^{29}	390	7.3	13
1675	Si^{30}	380	2.3	13
1680				18
1692	Si^{29}	1300	6.0	13
1701,1699	Si^{30}	790	2.9	13,18
1752	Si^{29}	1750	4.5	13
1774				8
1777	Si^{29}	650	6.2	13
1777	Si^{30}	1200	3.0	13

Proton Resonances in Natural Silicon
(900 to 1800 kev)

E_p(kev)$\pm$2	Width (kev)	Relative Yield .511 Mev	1.8 Mev	3.0 Mev
944	3.0	0.4		0.5
988	5.2	1.4		1.0
1035	9.0	0.8		0.0
1076	27.0	1.4		0.0
1104	5.4	0.8		0.0
1171	5.4	0.9		0.0
1214	6.0	1.8		1.2
1294	3.2	1.7	0.5	0.0
1310	6.0	2.0	2.1	1.3
1334	9.0	4.9	3.8	2.0
1377	13.3	$\not$	*	1.1
1399	2.4	$\not$	3.0	2.6
1407	6.3		2.8	
1488	10.0	$\not$		3.0
1498	4.3	$\not$		1.0
1518	4.5	$\not$		1.8
1527	5.4	$\not$		0.9
1531	*	$\not$		0.0
1655	$\sim$ 50.0	150		$\sim$ 25
1695	9.7	$\not$		*
1755	8.1	0.0		0.7
1781	13.0	$\not$		2.0

$\not$ .511 Mev Bias indication of presence
* Statistically unresolved

Table III

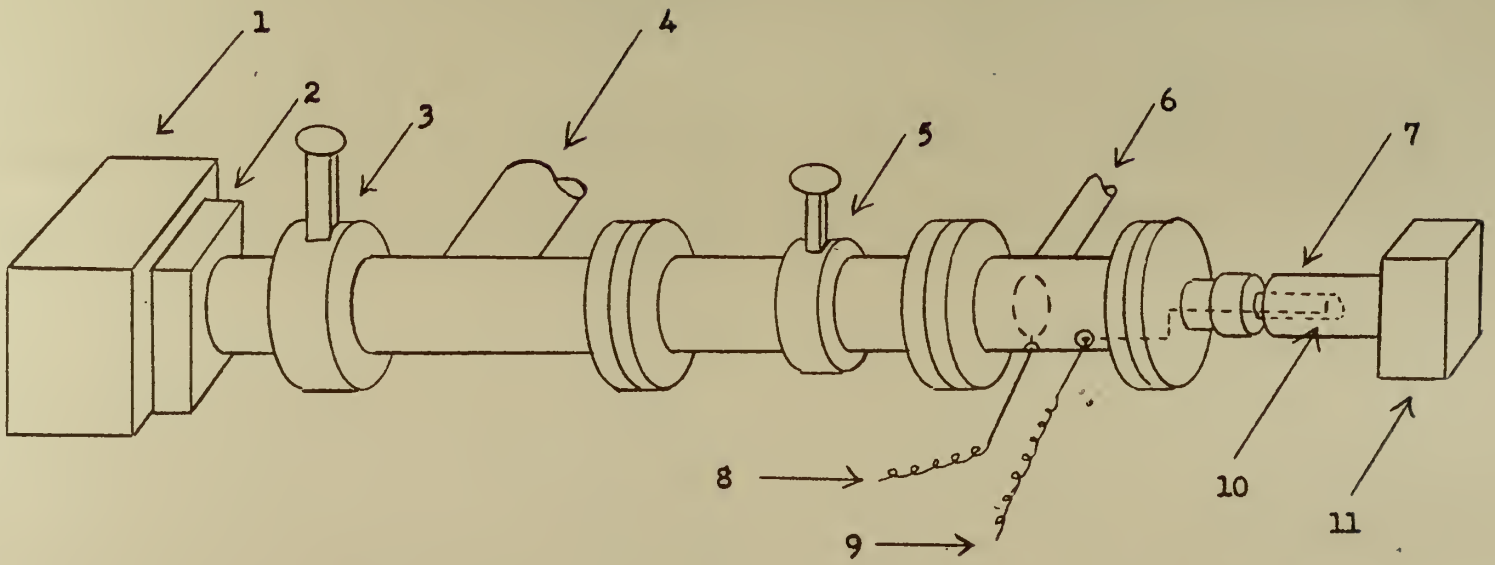

1. Slit system
2. Beam shutter assembly
3. Valve
4. To auxiliary vacuum system
5. Valve
6. To roughing valve and fitting
7. NaI(Th) crystal and photomultiplier
8. Faraday Cage wire
9. Target current wire
10. Target
11. Pre-amplifier

Fig. 1

Diagram of Target Section

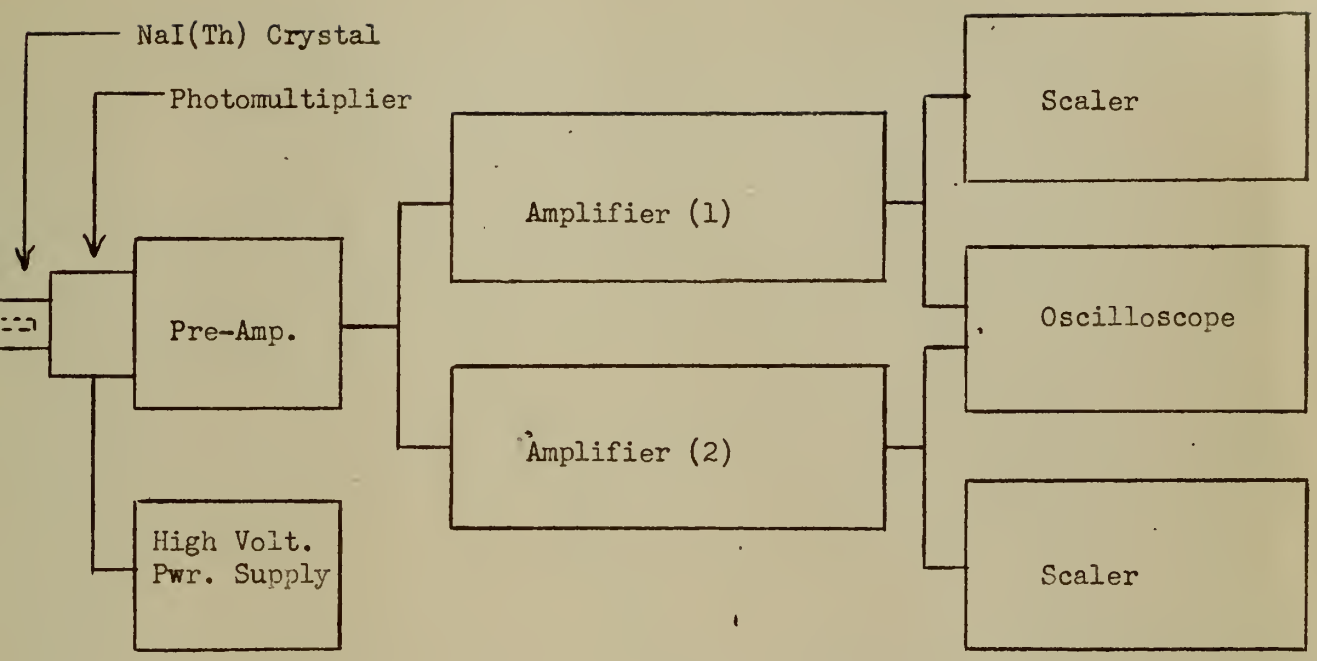

High Voltage Power Supply - Atomic Instruments Co., Model 306
Amplifier (1) - Hamner Electronics Corp., Non-overloading, Model N302
Amplifier (2) - Atomic Instruments Co., Non-overloading, Model 215
Scalers - Atomic Instruments Co., Glow-tube scaler, Model 988
Oscilloscope - Textronix Corp., Cathode-ray oscilloscope, Type 514AD

Figure 2

Block Diagram of Detection Equipment

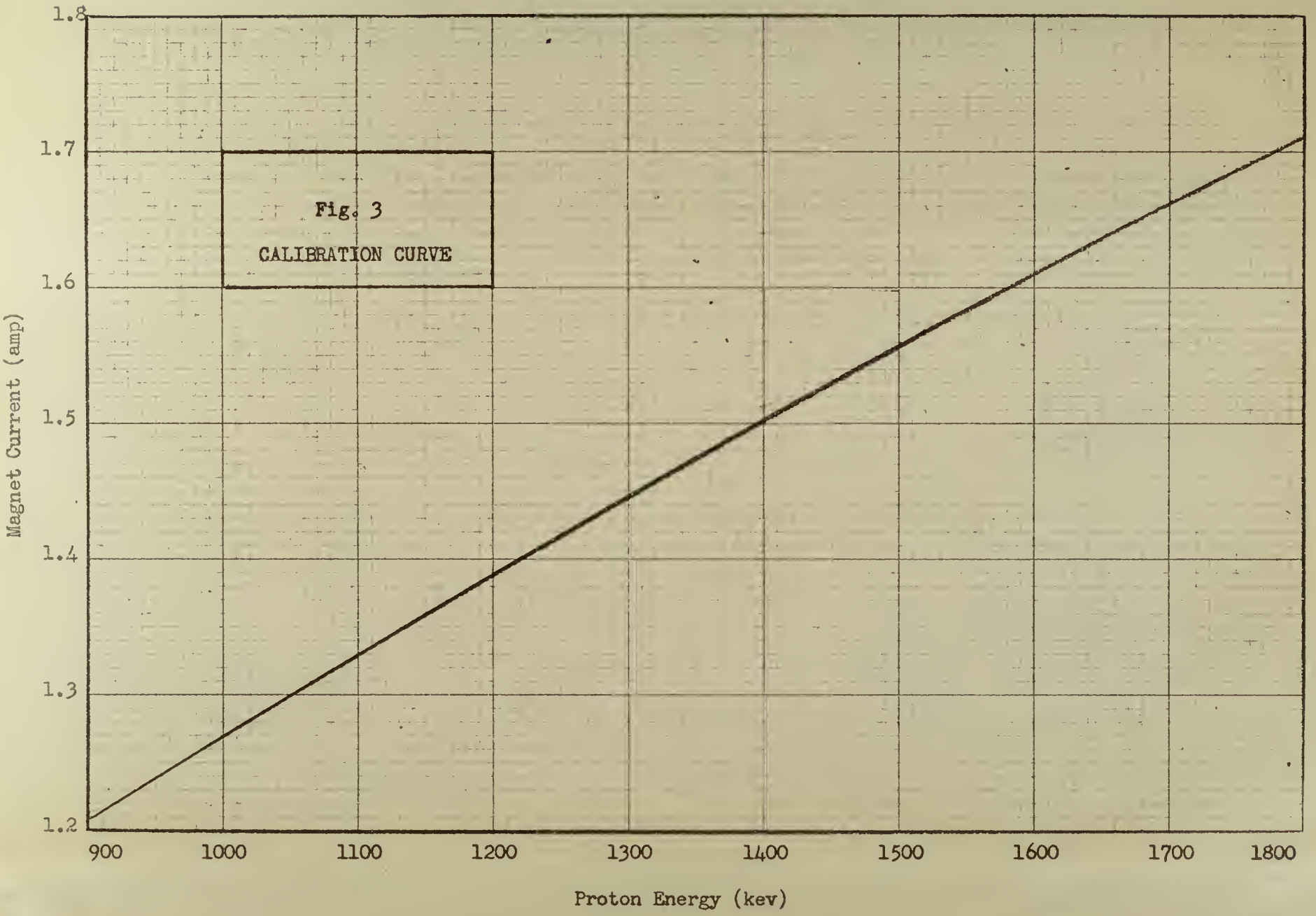
Fig. 3
CALIBRATION CURVE
Magnet Current (amp)
1.8
1.7
1.6
1.5
1.4
1.3
1.2
900
1000
1100
1200
1300
1400
1500
1600
1700
1800
Proton Energy (kev)

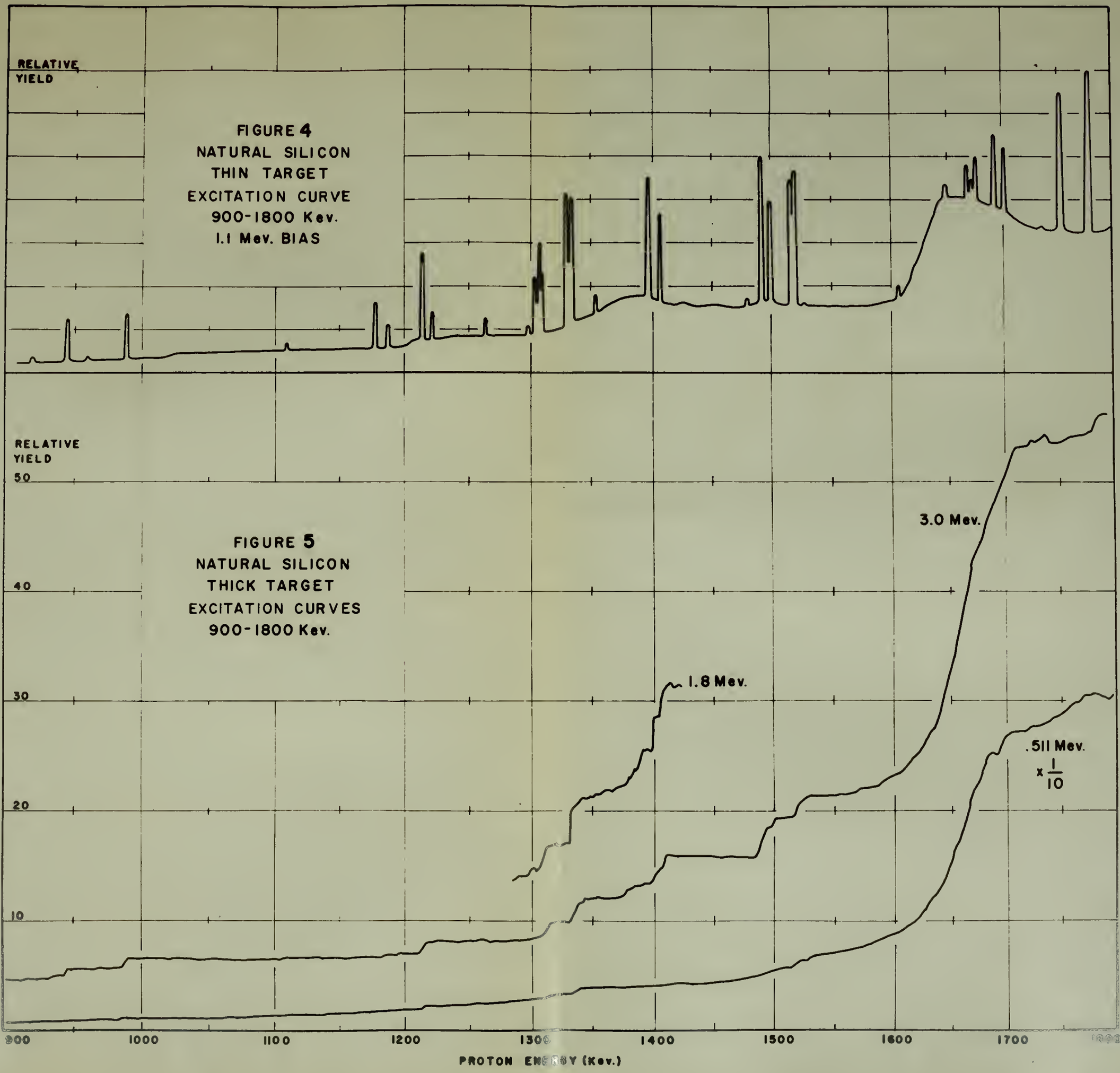
RELATIVE YIELD
FIGURE 4
NATURAL SILICON
THIN TARGET
EXCITATION CURVE
900-1800 Kev.
1.1 Mev. BIAS
RELATIVE YIELD
50
40
30
20
10
FIGURE 5
NATURAL SILICON
THICK TARGET
EXCITATION CURVES
900-1800 Kev.
3.0 Mev.
1.8 Mev.
.511 Mev.
x 1/10
900
1000
1100
1200
1300
1400
1500
1600
1700
PROTON ENERGY (Kev.)

FIGURE 6
EXCITATION CURVE 1300-1530 Kev.

FIGURE 7
EXCITATION CURVE 1550-1780 Kev.